EFFECT OF THE CRYSTALLOGRAPHIC ORIENTATION ON PHOTOVOLTAIC PROPERTIES OF p-GaP ELECTRODES

Ivo JAKUBEC[a1], Jiri VONDRAK[a2], Jana BLUDSKA[a3] and Ladislav PEKAREK[b]

[a] *Institute of Inorganic Chemistry, Academy of Sciences of the Czech Republic, 160 00 Prague 6, Czech Republic; e-mail: [1] jakubec@iic.cas.cz, [2] vondrakj@iic.cas.cz, [3] bludska@iic.cas.cz*

[b] *Institute of Physics, Academy of Sciences of the Czech Republic, 180 40 Prague 8, Czech Republic*

Received September 18, 1996
Accepted October 15, 1997

Hydrogen evolution from aqueous solutions on the p-gallium phosphide electrodes was studied by means of cyclic voltammetry and impedance spectroscopy. The semiconductor properties of the material, and consequently the efficiency of water photolysis, are affected by the crystallographic orientation of the photocathode surface.

Key words: p-Gallium phosphide; Photoelectrochemistry; Water photolysis; Semiconductors.

During the last period, photochemical evolution of hydrogen on semiconductor electrodes has been the object of intensive research in order to develop alternative, ecologically clean energy sources. Gallium phosphide (GaP) represents one of the materials which have been investigated for applications in photoelectrochemical (PEC) solar cells.

The absorption of a photon of the energy equal or greater than the band gap energy, E_g, on the semiconductor–electrolyte junction allows an electron to be transferred from the valence band to the conduction band. When the conversion efficiency has been evaluated for semiconducting materials with different band gaps, the maximum efficiency was found at $E_g \approx 1.4$ eV (ref.[1]). Therefore, the conversion efficiency of p-GaP at $E_g = 2.25$ eV is not optimum but it offers voltage reserve to compensate the overvoltage, and the use of p-GaP photocathodes seems to be promising[2,3]. Moreover, the GaP can be used as a component of tandem photoelectrodes. According to the theoretical predictions, these photoelectrodes, composed from 2–3 materials with different E_g, can absorb as much as 90% wavelengths of the total sun spectrum and their efficiency was estimated to be about 30% at air mass conditions equal to 1.5. The binary structure n-InP/p-$In_{0.5}Ga_{0.5}P$ is currently investigated as one of the most promising structures[4].

To reach a sufficient efficiency of the process, it is necessary to optimize the conditions of the electrolysis. The aim of this study is to report some new experimental data concenrning the effect of the crystallographic orientation of p-GaP electrode surface on the efficiency of water photolysis.

EXPERIMENTAL

Preparation of GaP Photocathodes

Polycrystalline GaP was synthesized from gallium (5N5) and phosphorus (6N) by the horizontal Bridgman method combined with the high temperature zone[5].

The p-GaP single crystal doped by zinc was grown by the liquid encapsulated Czochralski technique in the MSR6R apparatus (Metal Research LtD., G. B.). Parameters of the single crystal were the following: The specific resistivity of $4.8 \cdot 10^{-1}\ \Omega\ \mathrm{cm}^{-1}$, the Hall mobility of $41.6\ \mathrm{cm}^2\ \mathrm{V}^{-1}\ \mathrm{s}^{-1}$ and the hole concentration of $3.0 \cdot 10^{17}\ \mathrm{cm}^{-3}$.

GaP crystals form the zincblende-type structure which has two face centered cubic sublattices mutually shifted by the translation $t\ (\frac{1}{4}, \frac{1}{4}, \frac{1}{4})$. Four types of the crystallographic orientation of surface planes, namely cubic (100), tetraedrical $(111)_a$ and $(111)_b$, and rhombododecaedrical (110) were chosen to study the effect of the surface orientation on hydrogen photoevolution. The $(111)_a$ and $(111)_b$ orientations differ in occupation of the surface planes which contain only gallium and phosphorus, respectively, and atoms of the other kind are hidden beneath them. In addition, the behavior of a polycrystalline material was investigated.

To prepare electrodes with the (100), $(111)_a$, $(111)_b$, and (110) surface crystallographic orientations, the single crystal was oriented with the accuracy of 0.3° by means of X-ray diffraction and sliced. The average thickness of an electrode disk was 440 ± 15 μm. After slicing, the frontal electrode plane was brushed and polished in a mechanico-chemical way[5]. The $(111)_a$ and $(111)_b$ surface orientations were discerned by an etching procedure[5], where the more reactive $(111)_b$ surface plane had been polished while only dislocations had been etched on the $(111)_a$ surface plane.

Finally, the ohmic contact Au/Zn/Au was made by the sequential vacuum evaporation and its resistance was found to be about $10^{-1}\ \Omega$.

Electrochemical Measurements

Photoelectrochemical experiments were carried out at room temperature in a cell consisting of two compartments separated by a sintered glass disc. The working electrode together with a reference saturated calomel electrode (SCE) were placed in compartment separated from platinum counter electrode. Aqueous solution of 3 M HCl (purity for semiconductors) was used as an electrolyte. The light source was a 100 W tungsten–halogen lamp with the light flow of $0.02\ \mathrm{W}\ \mathrm{cm}^{-2}$. The light beam was passed through a water filter to absorb heat radiation. The cell was placed in a metallic screening chamber to eliminate any stray light from other sources.

Potentiostat PAR 263 with a lock-in amplifier model 5210 (EG&G) controlled by a computer was used for the electrochemical experiments.

Voltammetric measurements were performed in the potential range from 0.2 to –0.6 V *vs* SCE at the scan rate of $1\ \mathrm{mV}\ \mathrm{s}^{-1}$. The electrode area was of $1\ \mathrm{cm}^2$. Experimental data were recorded in the form of *i*–*E* curves.

The impedance spectra were measured without illumination in the potential range from 0.2 to –0.7 V *vs* SCE in 0.1 V steps with the amplitude of ac component of 5 mV and the range of frequency of 10 kHz–0.1 Hz. The Boukamp software EQUIVCRT (EG&G) was used for identification of the components of impedance spectrum.

RESULTS

Cyclic Voltammetry Under Illumination

Typical voltammograms recorded under illumination are shown in Fig. 1. The voltammograms of the (100) and (110) electrodes show waves at about –0.2 V corresponding to the photoevolution of hydrogen. The voltammogram for the $(111)_a$ electrode indicates only the electrochemical evolution of hydrogen and no photoeffect. The efficiency of the hydrogen photoevolution on the $(111)_b$ photocathode appears to be rather low. In comparison with the (100) and (110) electrodes, the onset of photocurrent on the $(111)_b$ photocathode is shifted towards more negative potentials and its maximum is several times lower.

Surprisingly, the photocurrent of the polycrystalline electrode is comparable with the photocurrents of the (100) and the (110) single crystal electrodes.

Cyclic Voltammetry Without Illumination

The current densities measured without illumination correspond to the electrochemical evolution of hydrogen (Fig. 2). The exchange current densities i_0 and the Tafel constants b were estimated from the linear sections of the cathodic branches of voltammograms, plotted in semilogarithmic scale (Fig. 3). The data are given in Table I together with the values of current densities at the vertex potentials, i_{H_2}, taken from the respective voltammograms in Fig. 2.

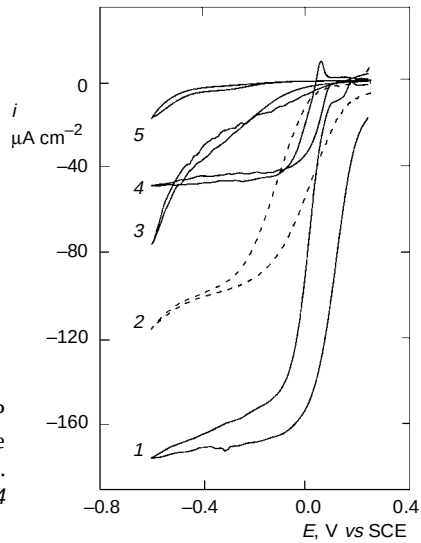

FIG. 1
Effect of the crystallographic orientation of p-GaP electrodes on photoevolution of hydrogen. Electrolyte 3 M HCl, scan rate 1 mV s^{-1}, illumination 0.02 W cm^{-2}. Electrode orientations: *1* (100), *2* (110), *3* $(111)_a$, *4* polycrystalline, *5* $(111)_b$

The Admittance Spectra

Two series of admittance spectrum in a three-dimensional representation are shown in Figs 4 and 5 where the modulus of admittance in a logarithmic scale is plotted against the logarithm of frequency in the whole potential range. Typical spectra of the $(111)_b$ electrode (Fig. 4) and those of the polycrystalline sample (Fig. 5) were chosen.

An equivalence circuit, displayed in Fig. 6, was used for their interpretation. It consists of parallel combination of the polarization resistance R_p with a series connection of a capacitance C with a constant-phase element. This element appears as a result of spatial processes, such as non-stationary diffusion flow, charge-controlled processes with time constants continuously spread in a broad frequency range, and charging of the double layer capacitance of an infinitely thin porous polarized electrode. The capacitance C_s consists of two elements in series, *i.e.* the capacitance of the double layer on the solution side and the capacitance of the Mott-Schottky barrier on the semiconductor side. However, the effect of the latter prevails in the series.

At higher frequencies, above 10–50 Hz, all spectra in Fig. 4 exhibit a capacitive behavior with the phase angle close to 90° and a monotonous rise of the admittance

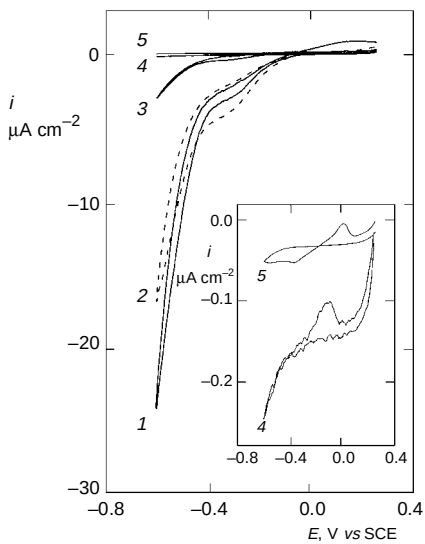

FIG. 2 *E*, V *vs* SCE

Effect of the crystallographic orientation of p-GaP electrodes on electrochemical hydrogen evolution. Electrolyte 3 M HCL, scan rate 1 mV S^{-1}, without illumination. Electrode orientations: *1* $(111)_a$, *2* $(111)_b$, *3* (110), *4* (100), *5* polycrystalline. Inset: *4* (100), *5* polycrystalline

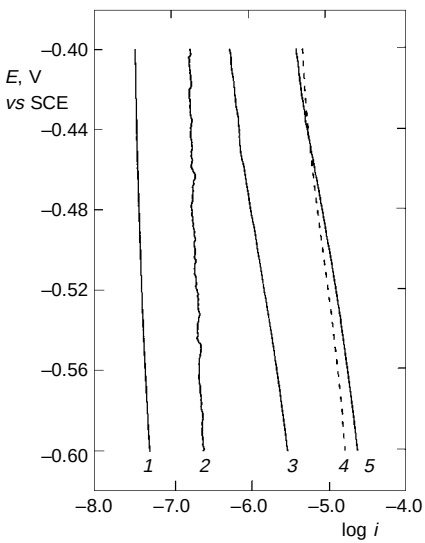

FIG. 3

Electrochemical evolution of hydrogen on p-GaP electrodes (Tafel plot). Electrolyte 3 M HCl, scan rate 1 mV s^{-1}, without illumination. Electrode orientations: *1* polycrystalline, *2* (100), *3* (110), *4* $(111)_b$, *5* $(111)_a$

TABLE I

Properties of GaP electrodes: E_{FB} is the flat band potential, n is the hole concentration, R_p is the polarization resistance, b is the Tafel constant, i_0 is the exchange current density and i_{H_2} is the current density at the vertex potential from voltammograms in Fig. 2

Electrode p-GaP	E_{fb} V	$n \cdot 10^{17}$ cm^{-3}	R_p kΩ	b V	i_0 A cm^{-2}	i_{H_2} A cm^{-2}
(100)	0.17	6.9	175	1.07	$6.74 \cdot 10^{-8}$	$2.5 \cdot 10^{-7}$
(110)	0.28	2.1	23	0.26	$1.41 \cdot 10^{-8}$	$3.0 \cdot 10^{-6}$
$(111)_a$	–	–	15	0.24	$8.60 \cdot 10^{-8}$	$2.5 \cdot 10^{-5}$
$(111)_b$	0.12	32.5	32	0.33	$2.81 \cdot 10^{-7}$	$1.7 \cdot 10^{-5}$
Polycryst.	0.76	140	1 220	1.08	$1.35 \cdot 10^{-8}$	$5.0 \cdot 10^{-8}$

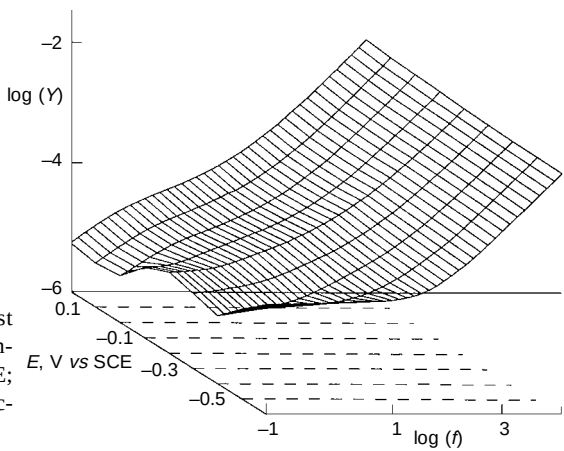

FIG. 4

Modulus of admittance plotted against frequency (in logarithmic scale). Potential range: from +0.2 to –0.6 V *vs* SCE; frequency range: 0.1 Hz–10 kHz; electrode orientation $(111)_b$

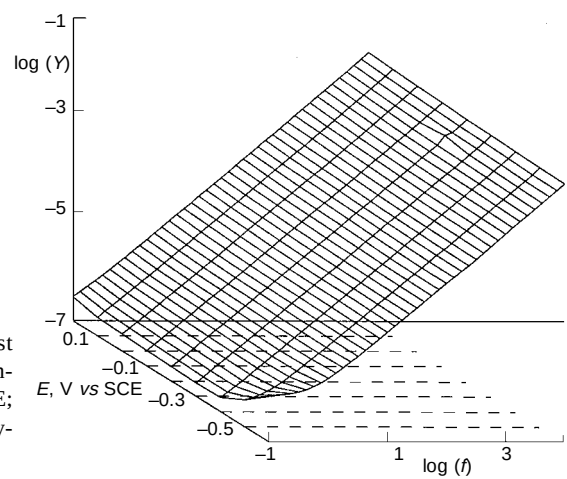

FIG. 5

Modulus of admittance plotted against frequency (in logarithmic scale). Potential range: from +0.2 to –0.6 V *vs* SCE; frequency range: 0.1 Hz–10 kHz; polycrystalline sample

modulus proportional to frequency. At low frequencies, below 10 Hz, the admittance approaches a constant value corresponding to the polarization resistance of hydrogen evolution if the potential is lower than –0.3 V, *i.e.*, in the range of hydrogen evolution. Moreover, we can see a resistive component with a maximum at –0.3 V and a constant phase component in the whole potential range (Fig. 4).

The behavior of the polycrystalline electrode is less complex. Nothing more than a polarization resistance and a capacitance display the spectra of the polycrystalline electrode (Fig. 5).

Similar but less pronounced constant phase components appear on spectra of the (100) and (110) electrodes. In the case of the $(111)_a$ electrode, it becomes the prevailing component of admittance and indicates, together with rather low polarization resistance R_p, high rate of direct hydrogen evolution.

Mott–Schottky Behavior

As mentioned above, the high-frequency range (above 10–50 Hz) exhibits capacitative characteristics. The Mott–Schottky behavior was found for all investigated electrodes except the $(111)_a$ electrode (Fig. 7). The effective values of the flat-band potential E_{fb} and the charge carrier concentration n are given in Table I assuming the roughness factor of 1 and the relative permittivity $\varepsilon = 11.1$ (ref.[6]). Moreover, the semiconductor was supposed to be isotropic with respect to its dielectric properties, thus neglecting the effect of the crystallographic orientation on the value ε.

There is no large discrepancy between n and the nominal carrier concentration given for the p-GaP original single crystal, $3.0 \cdot 10^{17}$ cm^{-3} (ref.[5]).

Low-Frequency Components

Constant phase elements were found in the admittance spectra of all electrodes excluding the polycrystalline one as shown in Fig. 8. Their values pass through a maximum

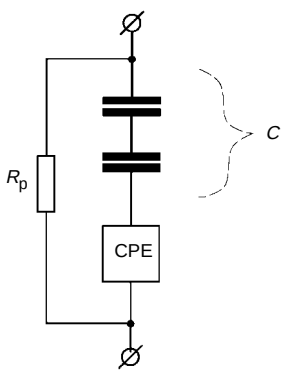

FIG. 6
Equivalence circuit: R_p is polarization resistance, C is a capacitance consisting of double layer and Schottky barrier capacitances, CPE is a constant phase element

between –0.4 and 0 V. The interpretation is rather difficult but the presence of moderately slow surface states on the electrode surface is indicated. A broadening of voltammograms is visible in the same potential range on some electrodes as an increase of distance between anodic and cathodic branches shown in Fig. 2.

Finally, a parallel resistance was found. As follows from Fig. 9, its values in the intermediate potential range are often rather high, thus indicating the absence of electrode faradaic processes, and high polarization of the electrode. This resistance decreases if potential reaches the range of hydrogen evolution (below –0.3 V).

DISCUSSION

The values of flat-band potentials of all the investigated GaP electrodes except the $(111)_a$ orientation are sufficiently above the region of hydrogen evolution, and photovoltaic hydrogen evolution is possible from this point of view.

The GaP electrode with $(111)_a$ orientation does not exhibit a typical Mott-Schottky behavior, and the semiconducting properties are suppressed by corrosion. Consequently, the efficiency of hydrogen evolution on this photocathode is low and its lifetime is short.

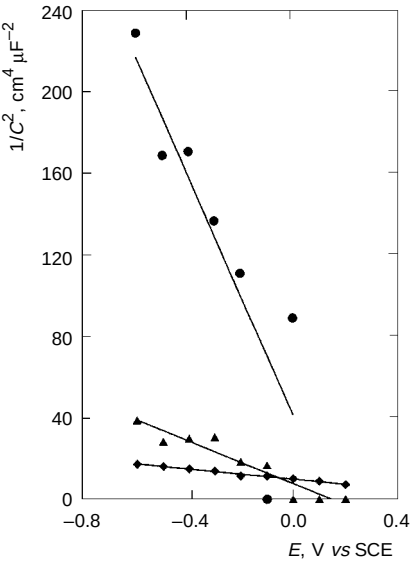

FIG. 7
Capacities of several GaP electrodes in Mott–Schottky representation. Frequency range 10 Hz–10 kHz. Orientation: ● (100), ▲ $(111)_b$, ◆ polycrystalline sample

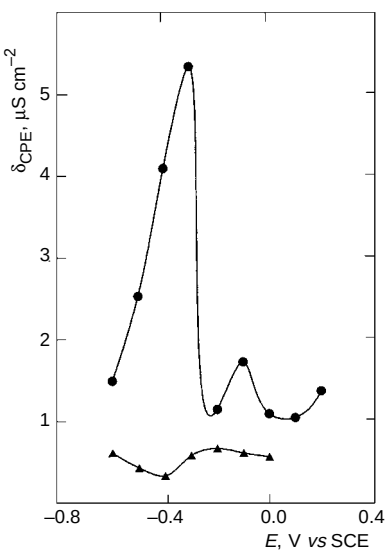

FIG. 8
Constant phase components δ_{CPE} with constant phase shift at $\omega = 1$. Frequency range below 10 Hz. Orientation: ● $(111)_b$, ▲ (100)

Electrochemical evolution of hydrogen is fairly easy on the GaP $(111)_b$ electrode where the process based on the reaction of surface phosphorus atoms can be expected:

$$\text{–P–OH} + \text{H}_2\text{O} + 2\,\text{e} \longrightarrow \text{–P–H} + 2\,\text{OH}^- \quad . \qquad (A)$$

If the lattice constant of GaP is 0.545 nm, then 1 cm^2 of an ideal surface contains $1.5 \cdot 10^{15}$ phosphorus atoms, requiring electric charge of 0.5 mC. The potential of that process is close to the equilibrium potential of hydrogen. Hence, it seems to be probable that the reaction of surface phosphorus atoms is an intermediate step of the hydrogen evolution. This reaction should be followed by the formation of molecular hydrogen according to the Tafel reaction of two adjacent H atoms:

$$\text{–P–H} + \text{H}_2\text{O} \longrightarrow \text{–P–OH} + \text{H}_2 \quad . \qquad (B)$$

This is in accordance with principles of electrocatalysis, and the constant phase element should be high in the range close to the equilibrium potential of hydrogen evolution, –0.24 V *vs* SCE.

The electrochemical evolution of hydrogen occurs below –0.3 V. The differences in the Tafel constant *b* should be explained easily by the differences of semiconductor properties. If the electrode is a typical p-type semiconductor, the main part of the voltage difference is located in the Schottky barrier inside the semiconductor and only lesser part contributes to supply potential for the hydrogen overvoltage itself. This

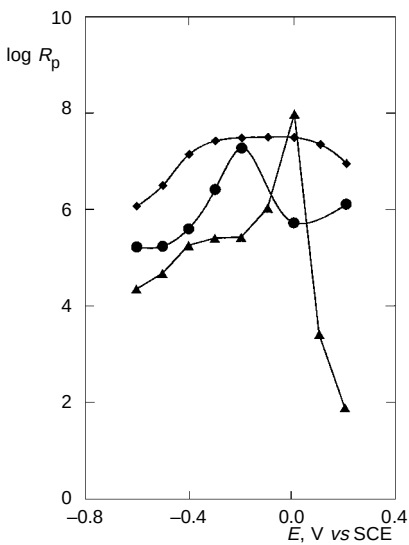

FIG. 9
Polarization resistance R_p, (Ω) in a logarithmic scale. Frequency range below 10 Hz. Orientation: ● (110), ▲ $(111)_b$, ◆ polycrystalline

corresponds to the electrode admittance with prevailing behavior of a capacitor, the capacitance of which is by 2–3 order of magnitude lower than that of electrode double layer on the electrolyte side of the phase boundary. Therefore, any faradaic process in blocking direction (towards negative potentials) is difficult, and the apparent constant *b* would be fairly high. In contrast, its value decreases considerably on the $(111)_b$ electrode where the semiconducting properties are short-circuited by adsorbed hydrogen, and the reaction is catalyzed by the monolayer of P–H groups.

The photovoltaic efficiency of the polycrystalline electrode is surprisingly high. Fairly high rate of hydrogen evolution should be ascribed to greater number of point line defects, integrain connections and similar defects on this sample in comparison with single crystal samples used otherwise. These defects should enhance the electrocatalytic activity for hydrogen evolution, and it should prevail over the inhibition by shortening life-time of electron-hole pairs in the semiconductor, generated by light absorption. The shift of the flat-band potential towards more positive values also indicates some enhancement of photocurrent generation in the Schottky barrier of polycrystalline sample.

With an exception for the $(111)_a$ surface, all investigated electrodes show properties as Schottky-type barrier electrodes and generate the photovoltaic effect. Efficiency of photolysis does not increase remarkably if salts of noble metals are added into electrolyte. This is manifested in Fig. 10 where the photocurrents of the (110) electrodes both in the absence (curve *2*) and in the presence of H_2PtCl_6 (curve *1*) are plotted. It seems that the platinum addition supports rather the direct electrochemical evolution of hydrogen than photoevolution on p-GaP cathodes in contrast to p-InP electrodes where

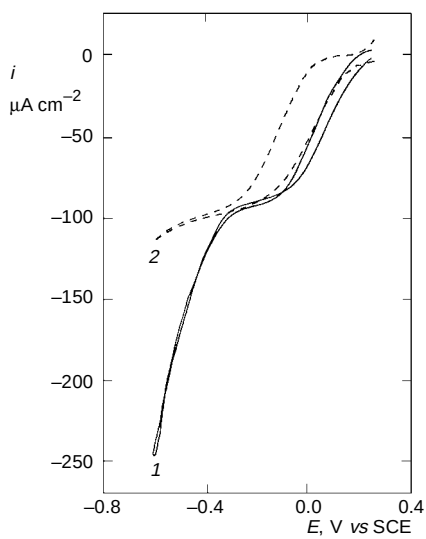

FIG. 10
Effect of platinum catalysis on hydrogen photoevolution on p-GaP electrodes. Electrolyte 3 M HCl, scan rate 1 mV s^{-1}, illumination 0.02 W cm^{-2}, electrode area 1 cm^2, electrode orientation (110); concentration of Pt *1* 7 . 10^{-5} mol l^{-1}, *2* 0 mol l^{-1}

the presence of platinum catalyst significantly restrains photocorrosion and increases the efficiency of the hydrogen photoevolution[7].

The crystallographic orientation markedly affects the electrochemical behavior of p-GaP semiconducting electrodes. With an exception for the $(111)_a$ orientation, the p-GaP electrodes are capable of hydrogen photoevolution in the applied potential region. Remarkably good activity of a polycrystalline electrode is explained by the electrochemical activity of surface defects.

The financial support of the Grant Agency of the Czech Republic (Grant No. 104/95/0034) is gratefully acknowledged.

REFERENCES

1. Fischer C. F.: *Festkorperprobleme*, Vol. 14. Pergamon Press, Braunschweig 1974.
2. Vanmaekelbergh D., Marin F. I., Vandelagemaat J.: *Ber. Bunsen-Ges. Phys. Chem.* **1996**, *100*, 616.
3. Flaisher H., Tenne R., Halmann M.: *J. Electroanal. Chem.* **1996**, *402*, 97.
4. Guochang L.: *Sol. Energy Mater. Sol. Cells* **1993**, *30*, 61.
5. Pekarek L., Jakubec I., Bludska J., Vondrak J. Mares J.: *Report MP-RP-4000/01/94*. Institute of Physics, Academy of Sciences of the Czech Republic, Prague 1994.
6. Bacher A. S., Jr.: *Phys. Rev.* **1968**, *165*, 917.
7. Jakubec I., Bludska J., Pekarek L., Vondrak J., Mares J.: *Collect. Czech. Chem. Commun.* **1995**, *61*, 77.